Direct Measurements of Temporal Wave Field Evolution in a Laboratory Tank and Comparison with Strongly Nonlinear Simulations

Lev Shemer[1], Alexey Slunyaev[2], Boris Dorfman[1]

[1]School of Mechanical Engineering, Tel-Aviv University, Tel-Aviv, Israel
Shemer@eng.tau.ac.il
[2]Institute of Applied Physics, RAS, Nizhny Novgorod, Russia
Slunyaev@hydro.appl.sci-nnov.ru

Abstract. The evolution along a tank of unidirectional nonlinear wave groups with narrow spectrum previously studied in [1] is compared with numerical simulations based on weakly, strongly and fully nonlinear models. Measurements of the instantaneous surface elevation within the laboratory tank were carried out using digital processing of video-recorded sequences of images of the contact line movement at the tank side wall. Records of the measured surface displacements variation were obtained along the entire tank at different instants. The accumulated set of experimental data enables to compare directly the experimental data with the results of numerical simulations based on conventional numerical models which describe wave field evolution in time.

Keywords: unidirectional wave groups, narrow-banded wave groups, laboratory experiment, wave measurement, video image processing, strongly nonlinear numerical simulation

1 Introduction

Theoretical studies of nonlinear water waves are often performed by solving temporal evolution models. Contrary to that, in the laboratory as well as in the field experiments surface elevation variation with time is usually recorded at fixed locations. Attempts are sometimes made to translate the measured by point sensors frequency spectrum into the corresponding wave number (or wave vector in the two-dimensional case) spectrum. However, direct quantitative comparison of the frequency and the wave number spectra can not be carried out in a consistent way; due to nonlinearity the wave field contains not only free but also bound (locked) components; nonlinearity also affects the dispersion relation among the wave number and the frequency.

Spatial forms of numerical models are thus natural when used to reproduce laboratory experiments and to carry out quantitative comparison with the

measurements. The spatial version of the modified nonlinear Schrodinger (or Dysthe) equation , as well as the spatial version of the Zakharov equation were suggested and successfully applied for the description of laboratory experiments [2-4]. Nevertheless, it should be stressed that (mainly for historical reasons) the variety of available "temporal" numerical models is more extensive.

In this paper instantaneous "snapshots" of the whole wave field in a laboratory tank are used for direct comparison of the laboratory measurements and the results of simulation employing different numerical models (ranging from weakly to fully nonlinear); all models describe the temporal evolution of the wave field. Recently, the laboratory results reported in the present paper were compared with the solutions of both temporal and spatial versions of the Dysthe equation [1], emphasizing the differences in the temporal and spatial approaches. In particular, it was found that for the Dysthe equation both approaches are capable of describing the nonlinear effects observed during the evolution of a narrow-banded wave field; the temporal and spatial forms of the Zakharov equation [3, 5], which is free of the narrow-band assumption, may be used for a more accurate estimate of wave dynamics. It was also stressed in [1] that due to the difference between the phase and the group wave velocities, the separation between the free and the bound modes is much more pronounced when the spatial wave evolution (and, respectively, the frequency spectrum) is considered. This is an additional consideration that makes the spatial formulation of the wave field evolution problem more convenient for practical purposes.

Section 2 describes the experimental facility and the method of retrieving and processing sequences of the recorded video images, that yields wave shapes along the whole tank at different instances. In Section 3 the initial conditions are presented that are used for laboratory wave generation, as well as for the initiation of the numerical simulations. Section 4 reports on the results of the numerical simulations within the frameworks of the temporal form of the Dysthe equation with full linear dispersion taken into account [6], the High-Order Spectral Method [7], and the fully nonlinear method for solving the Euler equations in terms of conformal mapping following [8].

2 Measurements and Experimental Data Processing

The experiments were performed in the wave tank that is 18 m long, 1.2 m wide and has transparent side walls and windows at the bottom which allow viewing of the flow from various directions. The tank is filled to mean water depth of $h = 0.6$ m. Waves are generated by a computer-controlled wavemaker system. The instantaneous contact line shapes were recorded by a CCD video camera at a rate of 30 fps. The size of each frame is 640 by 480 pixels. The field of view of the camera located one meter from the tank wall spans 50 cm along the tank (see Fig. 1), so that the pixel dimension is about 0.8 mm. The camera is placed on a carriage to enable imaging of different regions of the tank. Advantage is taken of the high repeatability of the wave field excited by the computer-generated driving signal. In each consecutive recording session, the carriage is shifted along the tank, so that slightly overlapping images of the contact line movement along the whole experimental facility are obtained. At each

camera location every frame of the recorded video clip was processed separately. The instantaneous surface elevation at any fixed location can also be measured by resistance type wave gauges made of 0.3 mm platinum wire.

An example of a recorded image is presented in Fig. 1. While the contact line can be clearly identified visually, the image contains numerous additional features such as the tank supporting beam, objects in the laboratory beyond the tank, reflections, etc. An effective algorithm was developed to extract quantitative information from the recorded video clips that contain thousands of images like that in Fig. 1. The initial window is built in the first image of the series around a point that constitutes the center of the searching area and is chosen at or in a close vicinity to the desired curve. The vertical coordinate of the interfacial curve for every horizontal location is defined as the weighted average of the pixel intensities along the vertical extent of the window. Once all vertical coordinates within the window are calculated, the contact line shape within the window is approximated by a second order polynomial using the least mean square fit on the array of the detected points. The window is then shifted forward by one pixel in the direction given by the slope of the contact line, and the process is repeated. This process continues until the whole image is covered. More detailed description of the method is given in [1, 9].

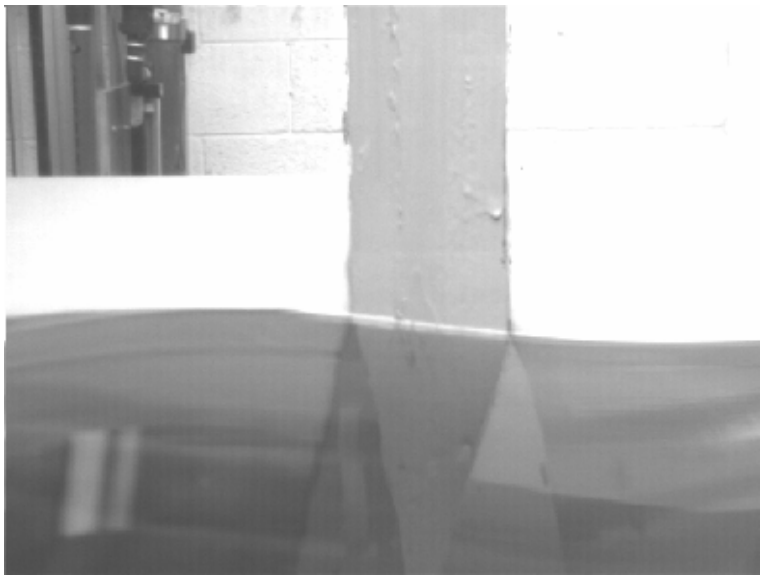

Fig. 1. An example of the contact line image.

The present experimental approach was validated extensively using conventional resistance wire gauges at a number of locations along the tank and comparing with the data simultaneously acquired at the same distance by image processing technique. The difference between the instantaneous values of the surface elevation measured by the wave gauge located close to the tank's wall and by video image processing at various distances from the wavemaker always remains well below 1 mm and does not exceed the deviation between the outputs of different probes, see [9].

3 Initial Conditions

Laboratory experiments were performed for a wave group with Gaussian envelope generated by the wavemaker. The temporal variation of the surface elevation at the wavemaker has to the leading order the following form:

$$A(t) = A_0 \exp\left(-(t/mT_0)^2\right)\cos\omega_0 t \ , \tag{1}$$

where $\omega_0 = 2\pi / T_0$ (T_0 = 1.5 s) is the carrier wave circular frequency, A_0 = 22 mm is the maximum wave amplitude in the group, and the parameter m = 3.5 defines the width of the group. These parameters were chosen to enable nonlinear effects to become apparent.

The wave group satisfies the narrow-banded condition, $\Delta\omega / \omega \approx 0.54$, see [1], and also the deep-water condition $k_0 h \approx 5$, where k_0 is the carrier wavenumber, related to ω_0 through the deep-water linear dispersion relation, $\omega_0^2 = gk_0$; g is the acceleration due to gravity.

To start temporal wave simulation, the boundary condition (1) has to be transformed into the waveform at the initial instant, say t = 0. In [1], this transformation was done invoking the linear solution. A simpler approach is used here. Neglecting dispersion effects at distances corresponding to the length of the train, equation (1) leads to the following initial condition:

$$A(x, t=0) = A_0 \exp\left(-\left(\frac{x - x_0}{mT_0 c_{gr}}\right)^2\right)\cos k_0 (x - x_0) \ , \tag{2}$$

where $c_{gr} \approx 0.54$ m / s is the carrier wave group velocity. The equation (2) describes the instantaneous wave field at the leading order at the instant prior to the group entrance to the tank. Since the spatial extent of the initial group is 6.3 m, in (2) x_0=3.15 m.

To compute the actual surface elevation, bound wave correction for finite-depth water up to the 3rd order [10] were taken into account

$$\begin{aligned} \eta = &-\frac{1}{4h}|A|^2 - \frac{i}{32(kh)^2}\left(AA_x^* - A^* A_x\right) + \mathrm{Re}\left[A\exp(i\omega_0 t - ik_0 x) + \right. \\ &\left. + \left(\frac{k_0}{2}A^2 + \frac{i}{2}AA_x\right)\exp(2i\omega_0 t - 2ik_0 x) + \frac{3k_0^2}{8}A^3\exp(3i\omega_0 t - 3ik_0 x)\right], \end{aligned} \tag{3}$$

where $A(x, t)$ is the complex wave amplitude associated with the Dysthe equation. Transform (3) takes into account the first harmonic (the carrier wave), the bound waves at the 2nd and the 3rd harmonics, and the long-wave bound correction that is represented by the two first items in (3).

The velocity potential on the free surface, $\varphi(x, t)$, required for the strongly and fully nonlinear numerical codes, is given by:

$$\varphi = -\sqrt{g/k_0}\ \mathrm{Im}\left[A\exp(i\omega_0 t - ik_0 x)\right]\exp(k_0 \eta) \ . \tag{4}$$

4 Numerical Simulations

The temporal wave evolution was solved within three numerical models: i) the Dysthe equation valid for deep water with full linear dispersion taken into account [6]; ii) the finite-depth High-Order Spectral Method of Dommermuth and Yue [7] (hereafter referred to as DY) with the nonlinear parameter $M = 6$; and iii) by means of the conformal mapping approach, developed by Dyachenko and Zakharov [8] (DZ hereafter), which is a fully-nonlinear spectral method for solving the potential Euler equations; its infinitively deep water version was used. All these models are derived for potential equations of ideal hydrodynamics and describe the linear dispersion without limitations (although different assumptions regarding the water depth are applied). The Dysthe model describes the evolution of wave group envelope under the assumption of weak nonlinearity and narrow spectrum. The DY model with $M = 6$ is often considered as a fully-nonlinear, since it takes into account higher-order nonlinear interactions. No details of the codes can be given here and may be found in the appropriate references; all are implemented using traditional approaches.

In the Dysthe simulations, (2) was used as the initial condition. To start simulations in the DY and DZ codes, nonlinear bound corrections (3) were taken into account, and the velocity potential was defined according to (4).

Surface displacement wave profile at $t = 0$, as well as the experimental measurements and the results of numerical simulations for three instants, $t = 14$ s, $t = 16$ s and $t = 18$ s, are shown in Fig. 2. The maximum duration of the wave propagation is limited by the size of the tank. Free wave envelopes obtained by inversing numerically the transform (3) are shown correspondingly in Fig. 3. The free wave envelope at $t = 0$ is actually the Gaussian wave envelope defined by (2).

The modification of the wave group shape in the course of its propagation along the tank is evident; it is caused by both the dispersive and the nonlinear effects. The effect of nonlinearity is manifested in the change of spectral shape, as discussed in [1]. The general agreement between the computations according to all models applied here and the experiments is quite satisfactory, but not perfect. The observed discrepancy between the numerical simulations, especially between the strongly nonlinear (DY) and the fully nonlinear (DZ) solvers, suggests that the nonlinear effects are manifested quite strongly during the evolution. On the other hand, a relatively simple weakly nonlinear Dysthe equation proves to be an adequate tool to describe the experiment.

The following explanations may be suggested for the minor differences found between the experimentally measured and the simulated wave fields. The most likely source for the discrepancy is that the initial condition for the numerical experiments is not exact. The translation of the wavemaker movement in time at $x = 0$ that results in (1) to the initial spatial distribution (2) is only approximate and neglects both dispersion and nonlinearity effects during the group propagation over a distance corresponding to its length.

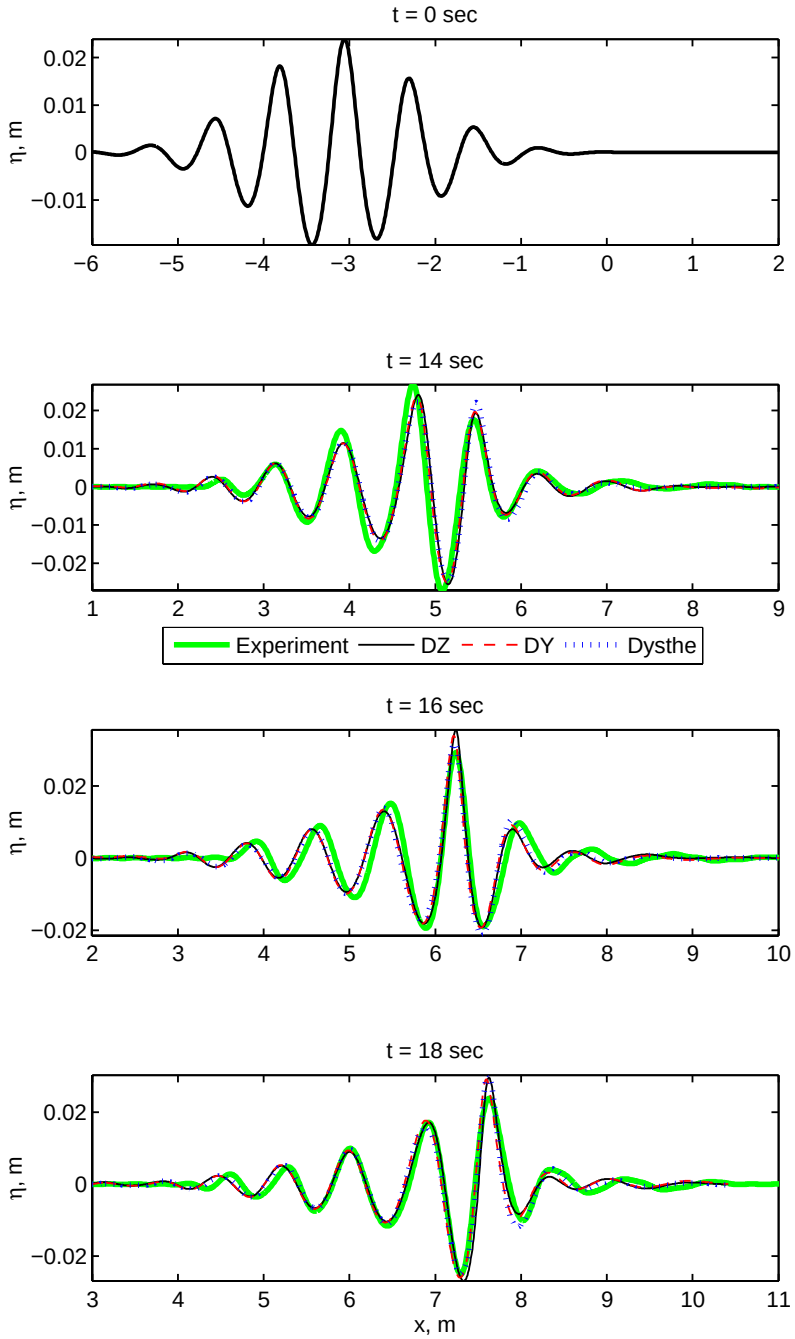

Fig. 2. Experimental (thick solid line) and simulated (thin solid line – DZ code, dashed line – DY code, dotted line – Dysthe code) surface displacement profiles at different instants.

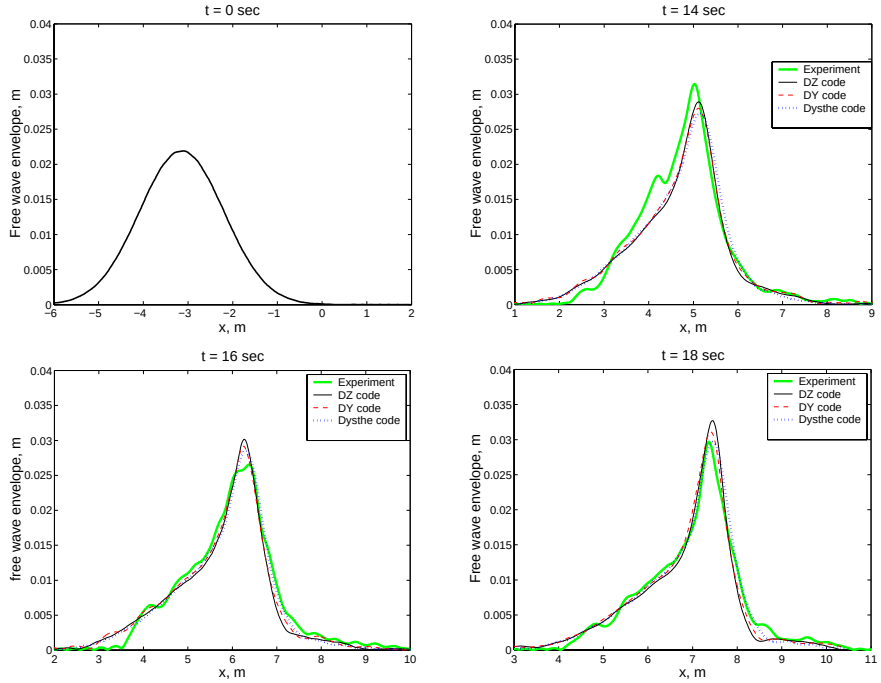

Fig. 3. Experimental and simulated free wave envelopes of surface displacement at different instants.

Comparison of those curves in Figs. 2 and 3 that correspond to the numerical simulations also suggests that the stronger is the nonlinearity of the model, the steeper individual waves it is capable to predict. Among the models employed in this study, the DZ model is the most (fully) nonlinear, the DY model with $M = 6$ describes up to 7-wave interactions, and the Dysthe equation takes into account only four-wave interactions.

Conclusion

The method of obtaining instantaneous distribution of surface wave displacement along the entire laboratory tank at various instances enables direct comparison of laboratory measurements with the results of numerical simulations performed within the framework of conventional models that describe temporal evolution of the nonlinear wave field. In this paper laboratory measurements of nonlinear wave dynamics of high-amplitude narrow-banded wave groups are quantitatively compared with the solutions of the weakly nonlinear Dysthe equation, the strongly nonlinear High-Order Spectral Method and the fully nonlinear Euler equations written in conformal variables. This approach provides a straightforward way to verify those

numerical models experimentally. In particular, to the best of our knowledge this is the first case when the solution of the Euler equations in conformal variables is compared with a laboratory experiment.

Acknowledgments. The research is supported by grant # 3-3573 from the Israel-Russia Cooperation Program, by grant # 964/05 from the Israeli Science Foundation (LS). The research for AS is supported by RFBR grants # 06-05-72011 and 08-02-00039, State Programme 2008-MO-04-06 and project Extreme Seas.

References

1. Shemer L., Dorfman B.: Experimental and numerical study of spatial and temporal evolution of nonlinear wave groups. Nonlin. Proc. Geophys. 15, 931-942 (2008).
2. Lo E., Mei C.C.: A numerical study of water-wave modulation based on a higher-order nonlinear Schrödinger equation. J. Fluid Mech. 150, 395-416 (1985).
3. Kit E., Shemer L.: Spatial versions of the Zakharov and Dysthe evolution equations for deep water gravity waves. J. Fluid Mech. 450, 201-205 (2002).
4. Shemer L., Kit E., Jiao H.-Y.: An experimental and numerical study of the spatial evolution of unidirectional nonlinear water-wave groups. Phys. Fluids 14, 3380-3390 (2002).
5. Zakharov V.E.: Stability of periodic waves of finite amplitude on the surface of a deep fluid. J. Appl. Mech. Tech. Phys. 9, 190-194 (1968).
6. Trulsen K., Kliakhandler I., Dysthe K.B., Velarde M.G.: On weakly nonlinear modulation of waves on deep water. Phys. Fluids 12, 2432–2437 (2000).
7. Dommermuth D.G., Yue D.K.P.: A high-order spectral method for the study of nonlinear gravity waves. J. Fluid. Mech. 184, 267-288 (1987).
8. Zakharov V.E., Dyachenko A.I., Vasilyev O.A.: New method for numerical simulation of a nonstationary potential flow of incompressible fluid with a free surface. Europ. J. Mech. B/Fluids 21, 283-291 (2002).
9. Dorfman B., Shemer L.: Video image-based technique for measuring wave field evolution in a laboratory wave tank, Maritime Industry, Ocean Eng. and Coastal Resources, 2, edited by: Guedes Soares C. and Kolev P.K., Taylor & Francis, London. 711–720 (2007).
10. Slunyaev A.V.: A high-order nonlinear envelope equation for gravity waves in finite-depth water. JETP 101, 926-941 (2005).